Bimetallic Particle Formation in Pt–Re/Al₂O₃ Reforming Catalysts Revealed by Energy-Dispersive X-Ray Spectrometry in the Analytical Electron Microscope

Rune Prestvik,[*,1] Bård Tøtdal,† Charles E. Lyman,‡ and Anders Holmen§

*SINTEF Applied Chemistry, N-7034 Trondheim, Norway; †Department of Physics, Norwegian University of Science and Technology, 7034 Trondheim, and SINTEF Applied Physics, N-7034 Trondheim, Norway; ‡Department of Materials Science and Engineering, Lehigh University, Bethlehem, Pennsylvania 18015-3195; and §Department of Industrial Chemistry, Norwegian University of Science and Technology, N-7034 Trondheim, Norway

The metal function of a commercial 0.3–0.3 wt% Pt–Re/Al₂O₃ catalyst was studied by scanning transmission electron microscopy (STEM) and energy dispersive X-ray spectrometry (EDX). Evidence for platinum–rhenium bimetallic particle formation in the reduced catalyst has been established. The degree of Pt–Re interaction is highly dependent on the conditions employed during catalyst pretreatment. The highest degree of Pt–Re interaction is obtained if the catalyst is not dehydrated prior to reduction. High-temperature N₂ treatment causes platinum oxide decomposition, sintering, and a low degree of Pt–Re interaction. The part of the rhenium not associated with platinum is possibly distributed on the surface of the alumina support as submicroscopic particles.   © 1998 Academic Press

INTRODUCTION

The superior catalyst stability resulting from the addition of rhenium to Pt/Al₂O₃ has been a subject of discussion since the introduction of the bimetallic catalyst in 1968 (1). Different theories concerning the role of rhenium in this catalyst system have been described (2–10), among which the idea of platinum–rhenium "alloy" formation (Pt–Re interaction) has been frequently discussed (6–11). Different conclusions, arriving from both chemical and physical characterization methods, have been made on whether bimetallic particles are formed or not. Due to the very high metal dispersions of these catalysts, direct evidence for Pt–Re interaction from physical characterization methods is difficult to obtain. The use of model catalysts with higher metal loadings is not necessarily representative of the commercial reforming catalyst. In addition, the influence of the catalyst pretreatment on the final state of the catalyst must also be considered. The literature concerning Pt–Re interaction in the Pt–Re/Al₂O₃ system has been reviewed elsewhere (12, 13).

In a previous study (13) the effect of catalyst pretreatment on the metal function was investigated using temperature-programmed reduction, TEM, hydrogen chemisorption, and model reactions. It was concluded that the degree of hydration of the catalyst prior to reduction, as defined by the drying temperature, strongly modifies the reducibility of rhenium and the extent of Pt–Re interaction in the reduced catalyst. When the catalyst is not dehydrated (drying temperature ≤250°C), platinum catalyzes the reduction of rhenium which is reduced at low temperature by a mechanism possibly involving rhenium oxide migration. Bimetallic particles of platinum and rhenium are formed. When the catalyst is further dehydrated (drying temperature 550°C), the rhenium oxide species become gradually less mobile resulting in higher reduction temperatures. Part of the rhenium is completely immobilized and is reduced at a temperature of about 600°C, typical for monometallic rhenium. Consequently less bimetallic interaction is achieved. The measured decrease in hydrogen adsorption when the catalyst was not dehydrated prior to reduction confirmed the above results (13). Similar results have been obtained by Isaacs and Petersen (14) who explained the lower H₂ uptake by a reduction of platinum–platinum pairs, required for dissociative adsorption, in the bimetallic phase.

The observed increase in hydrogenolysis activity (13) also served as an indication of increased degree of Pt–Re interaction as postulated by Augustine and Sachtler (15). These authors (15) explained the activity enhancement for the reaction by an intermediate heat of adsorption, between the two extremes of pure platinum and pure rhenium.

Although hydrogenolysis activity, hydrogen adsorption, and results from other methods indicate bimetallic particle formation, no direct evidence has so far been put forward. In fact, a recent TEM/EDX study (16) concluded after studying a commercial 0.3–0.3 wt% Pt–Re/Al₂O₃ catalyst (EUROPT 4) that rhenium was not at all associated with platinum metal. It was concluded that rhenium is evenly

distributed on the surface of the alumina support. The metal particles observed in that study were 2–3 nm in diameter. The authors did, however, suggest that the platinum particles observed accounted for only a small amount of the total platinum in the catalyst, the majority of platinum being TEM-unrecognizable.

Combined TEM/EDX analysis is a powerful technique for studying this kind of systems provided that the resolution is high enough to observe the majority of the particles. The present work deals with a study of the EUROPT-4 catalyst using the highest resolution STEM/EDX instrumentation available, allowing elemental analysis of multimetallic particles as small as 0.5 to 1.0 nm (17, 18). By plotting particle composition versus particle size, trends in the data are revealed that can not be offered by any other analytical method.

EXPERIMENTAL

Catalyst

The reforming catalyst was EUROPT-4 (0.3–0.3 wt% Pt–Re/γ-Al$_2$O$_3$) manufactured by Akzo. The chloride loading was 0.95 wt%. The commercial extrudates were crushed and sieved and the particles with the size of 0.25 to 0.60 μm were used. The as-received catalyst contained approximately 5 wt% water of hydration.

Catalyst pretreatment and reduction was done *ex situ* in a fixed-bed microreactor apparatus described elsewhere (12). All the gases used were purified by molsieves and O$_2$-traps. Five catalyst samples with different drying conditions prior to reduction were made. **Sample 1** was reduced directly without pretreatment by heating in H$_2$ (30 ml/min, g cat) from 20 to 480°C at a rate of 2.4°C/min. After 1 h reduction at 480°C the sample was cooled to ambient conditions. **Sample 2** was dried in air (30 ml/min, g cat) by heating at 0.8°C/min to 240°C. After 4 h drying, the sample was flushed with Ar for 5 min, then exposed to H$_2$ and heated 2.4°C/min to 480°C, where it was held for 1 h. **Sample 3** was dried in air by heating at 0.8°C/min to 550°C. After 4 h the sample was cooled to 400°C, flushed with Ar, exposed to H$_2$ and heated 0.8°C/min to 480°C, where it was held for 1 h. **Sample 4** was similar to sample 3, but dried in N$_2$ atmosphere instead of air. **Sample 5** was dried in N$_2$ by heating at 0.8°C/min to 680°C. After 4 h the sample was cooled to 400°C, flushed with Ar, exposed to H$_2$, and heated 0.8°C/min to 480°C, where it was held for 1 h. After reduction, the samples were cooled to ambient conditions and stored in bottles in a desiccator until STEM/EDX analysis was performed.

Electron Microscopy and EDX

The specimens were investigated in a dedicated STEM (VG HB-603) equipped with an EDX system (Oxford Link

eXL) with a windowless Si(Li) detector. The instrument was operated at 300 kV.

The samples were crushed in a mortar and the powder was dispersed dry onto a Ti grid coated with a holey carbon film. This proved to give less contamination than dissolving the powder in ethanol or hexane. In an attempt to improve the stability of the samples during examination under the electron beam, some grids were coated with a thin layer of carbon or metal. However, this led to increased difficulties in distinguishing the Pt/Re particles from the alumina support. In order to minimize hydrocarbon contamination, the specimens were kept in the microscope overnight before they were investigated. To minimize the contamination and increase the stability still further, some specimens were analyzed at temperatures near that of liquid N$_2$, but this technique led to increased mechanical instability and was abandoned.

Images were obtained in STEM mode with the annular dark-field detector, generally at a magnification of 2Mx–5Mx. The size of the particles was assessed by measuring with a ruler on the screen. The contrast was generally not very sharp, and the measured particle diameters must therefore be considered only approximate.

The EDX signals of the Pt/Re particles were obtained by focusing the electron beam on the particles and accumulating the spectra. Every 10 s the EDX accumulation was stopped and the microscope returned to imaging mode in order to keep track of the particle position. When it was no longer possible to detect a clear increase of the Pt or Re peaks, the EDX counting was stopped and the spectrum stored.

The spectra were later processed with the SIMPLEX procedure of the DTSA spectrum analysis program of National Institute of Standards and Technology (NIST). The number of counts in the ReLα and PtLα peaks were then used as net intensities I$_x$ in the formula:

$$\frac{C_{Pt}}{C_{Re}} = k_{Pt,Re}\frac{I_{Pt}}{I_{Re}}, \qquad [1]$$

where C is the mass fraction and k is the sensitivity factor (the "Cliff Lorimer k-factor"). We have assumed that the particles consisted of Pt and Re only, such that $C_{Pt} + C_{Re} = 1$, giving

$$C_{Pt} = \frac{k \cdot I_{Pt}}{I_{Re} + k \cdot I_{Pt}}. \qquad [2]$$

In the absence of a suitable Pt–Re standard, the k-factor was calculated (19) as $k = 1.05$ for analysis at 300 kV and at an X ray take-off angle of 20°.

RESULTS AND DISCUSSION

The catalyst samples (except for sample 1) have been extensively studied by other characterization methods

TABLE 1

Catalyst Sample Data Obtained in Previous Work (12)

Sample number	Drying atm/temp	H/Pt ratio[a]	C_1/C_3 mol ratio[b]	Crystallite size[c]	MCH conversion[d]
1	—	—	—	—	—
2	air 240°C	0.23	22	≤1 nm	41%
3	air 550°C	0.50	3	—	42%
4	N$_2$ 550°C	0.43	—	—	37%
5	N$_2$ 680°C	0.08	—	2–5 nm	27%

[a] Hydrogen pulse chemisorption at 20°C.

[b] Product from conversion of n-heptane at 505°C, 16 bar, WHSV = 10 h^{-1}, and H$_2$/n-C$_7$ = 10.

[c] TEM analysis (bright field contrast).

[d] Methylcyclohexane (MCH) conversion at 300°C, 1.1 bar, WHSV = 25 h^{-1}, and H$_2$/MCH = 40.

previously (13) and the results are summarized in Table 1. Sample 2 is characterized by low hydrogen uptake and high hydrogenolysis activity during n-heptane conversion, indicating high degree of Pt–Re interaction (13). Sample 3, on the other hand, gave higher hydrogen uptake and lower C_1/C_3 ratio (i.e., lower hydrogenolysis activity) during n-heptane conversion, thus indicating a lower degree of Pt–Re interaction. The MCH dehydrogenation results (platinum dispersion equivalent) and TEM suggest that the metal dispersions for samples 2 and 3 are equally high. Samples 4 and 5 were pretreated in N$_2$ atmosphere, causing lower metal dispersions and lower degrees of Pt–Re interaction in the reduced specimens due to platinum oxide decomposition and sintering during the pretreatment in
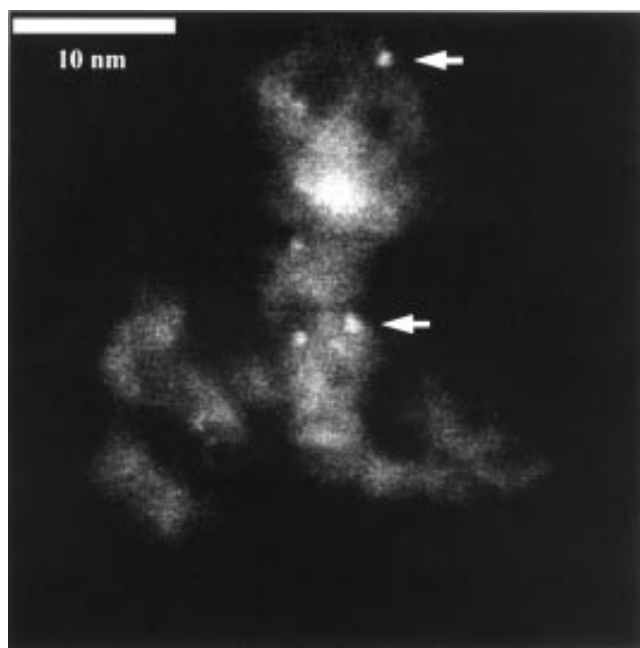

FIG. 1. Annular dark field image of a single piece of alumina containing many metal particles, sample 1. Arrows indicate metal particles.
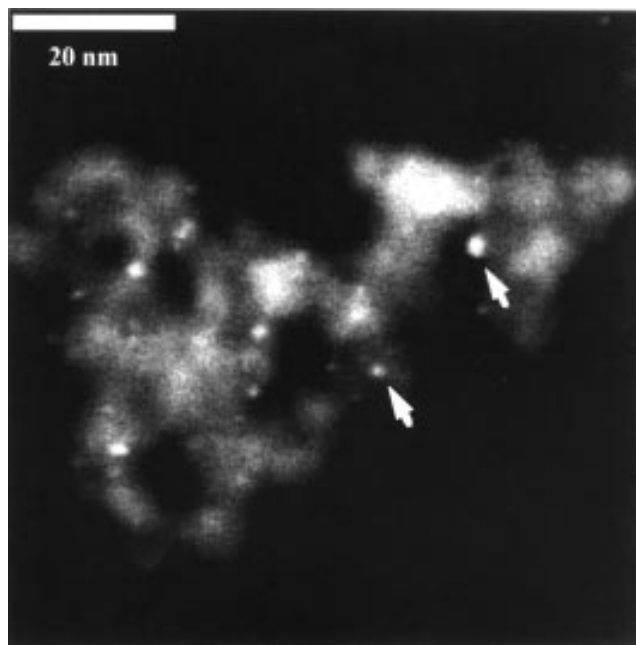

FIG. 2. Annular dark field image of a single piece of alumina containing many metal particles, sample 5. Arrows indicate metal particles.

nonoxidizing atmosphere (13). Sample 1 has been added to these previously studied samples since it is expected to represent a maximum in Pt–Re interaction.

The STEM analysis was performed by observing only thin layers (10–50 nm) of the supporting γ-Al$_2$O$_3$, thus simplifying metal particle detection. Typical annular dark-field STEM micrographs of samples 1 and 5 are shown in Figs. 1 and 2. The metal particles were observed as diffuse white spots caused by increased scattering relative to the alumina framework. The smallest metal particles detected were approximately 0.5 nm in diameter. Examples of collected EDX-spectra from metal particles of samples 1 and 5 are shown in Figs. 3 and 4. Platinum and rhenium signals
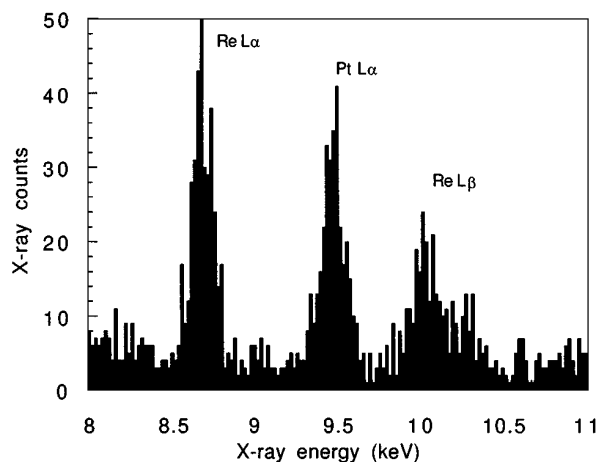

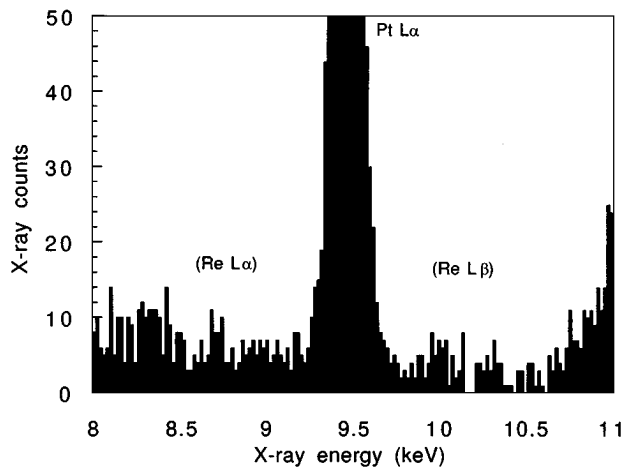**FIG. 3.** X-ray spectrum from a 0.8 nm particle in sample 1.

FIG. 4. X-ray spectrum from a 3 nm particle in sample 5.

originating from a single particle show that the metal particles are indeed bimetallic. When the electron beam was positioned on the alumina support outside a particle, both the platinum and rhenium signals dropped by an order of magnitude.

To obtain reliable EDX data, about 80 to 100 metal particles of each sample were analysed. The integrated counts from platinum and rhenium peaks, respectively, were isolated and the platinum fraction, $C_{Pt} = 1 - C_{Re}$, was calculated for each individual particle analysis. The measured platinum fraction varied considerably among the metal particles from individual samples. The particle composition-size distributions for the samples are shown in Figs. 5–9.
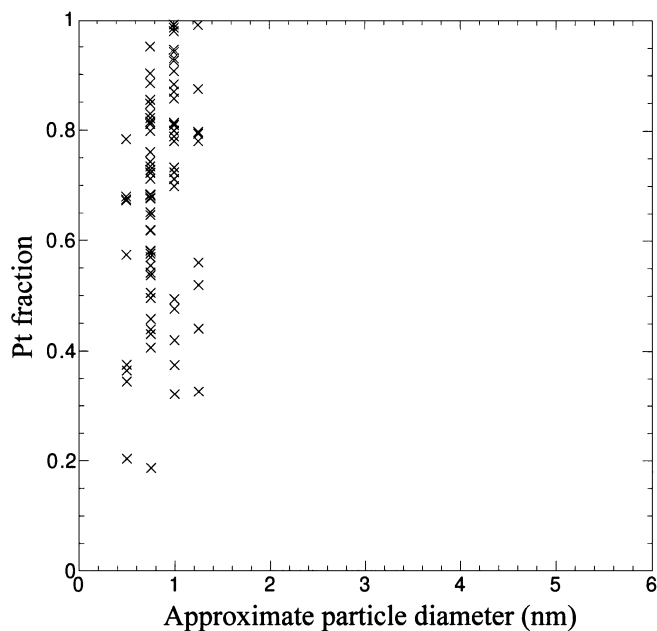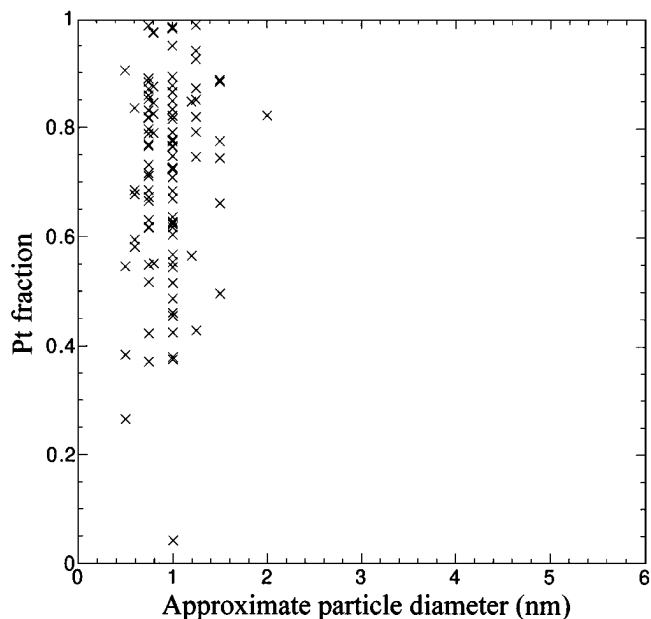

FIG. 6. Approximate particle diameter and measured Pt fraction of individual metal particles in sample 2.

In Table 2 the calculated intermediate value of platinum–rhenium particle composition (mass fraction) and the average metal particle diameters for each of the five samples are given.

Samples 1 and 2 show the highest degrees of Pt–Re interaction, with approximately 70% platinum and 30% rhenium as an average metal particle concentration (Table 2). This corresponds well with the previous results (13),
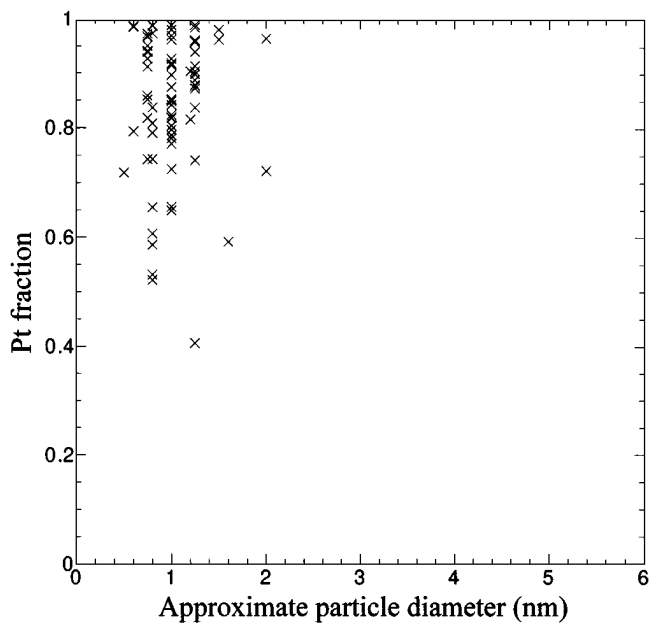

FIG. 5. Approximate particle diameter and measured Pt fraction of individual metal particles in sample 1.

FIG. 7. Approximate particle diameter and measured Pt fraction of individual metal particles in sample 3.
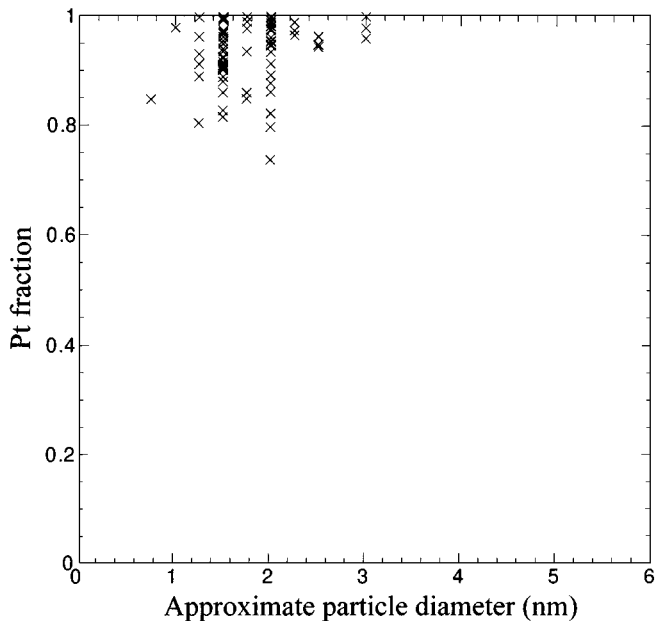
FIG. 8. Approximate particle diameter and measured Pt fraction of individual metal particles in sample 4.

suggesting high degrees of Pt–Re interaction for catalysts which were not dehydrated prior to reduction. A hydrated surface allows rhenium oxide to migrate to prereduced platinum atoms which supply atomic hydrogen for the reduction of rhenium. It follows from this mechanism that platinum and rhenium become intimately mixed after reduction. Similar particle compositions for sample 1 (not
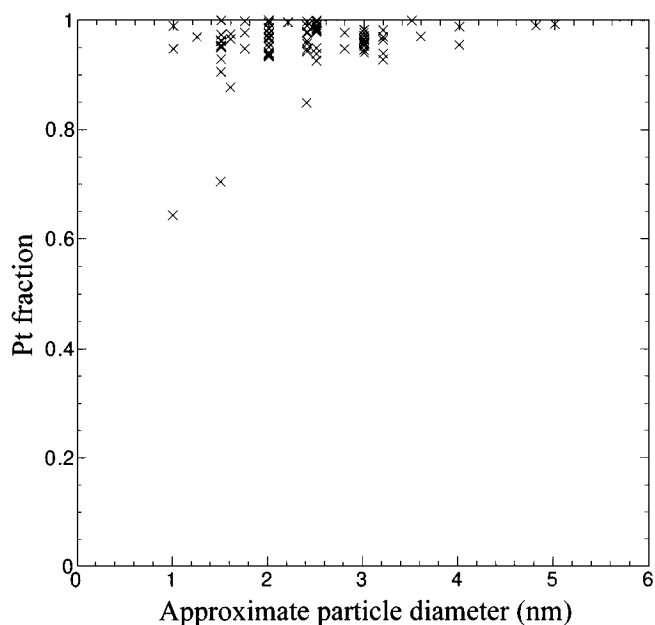

FIG. 9. Approximate particle diameter and measured Pt fraction of individual metal particles in sample 5.

TABLE 2

Average Pt and Re Mass Fraction and Average Particle Diameters for the Catalyst Samples Calculated from STEM/EDX Analysis of Individual Metal Particles in Each Sample

Sample number	Pt mass fraction, C_{Pt}	Re mass fraction, C_{Re}	Average particle diameter (nm)	Number of particles analyzed
1	0.68	0.32	0.9	86
2	0.71	0.29	1.0	100
3	0.85	0.15	1.0	78
4	0.94	0.06	1.8	85
5	0.96	0.04	2.3	86

dried) and sample 2 (air dried at 240°C) indicate that a catalyst dried at 240°C is still sufficiently hydrated to allow maximum rhenium oxide mobility and formation of bimetallic particles (13). The TPR-experiments of the previous investigation (13) suggested that rhenium in catalyst sample 2 is completely reduced and associated with platinum. The present EDX analysis of the alumina support outside the metal particles of sample 1 and sample 2 showed, in most cases, very small signals for platinum and rhenium.

For sample 3, dried in air at 550°C prior to reduction, the average particle composition is only about 15 wt% rhenium (Table 2). Thus, the degree of Pt–Re interaction is much lower compared to samples 1 and 2. Again, this corresponds well with the observed increase in hydrogen adsorption and lowering of the hydrogenolysis activity of the catalyst and is a result of lower rhenium oxide mobility on a dehydrated catalyst surface. While the amount of rhenium in the metal particles is lower than for samples 1 and 2, part of the rhenium is to be found elsewhere on the alumina support surface. From the previous TPR measurements (13), it was shown that some rhenium is reduced at high temperature while the rest stays in the oxidized state. The present EDX elemental analysis did not provide oxide state differentiation, but the analysis of the support away from the metal particles of sample 3 did sometimes give small rhenium signals, although not much larger than the noise in the background level. Anyway, no pure rhenium particles were discovered in sample 3, or in any of the other samples. This suggests that the part of rhenium which is not associated with platinum is distributed on the surface of the alumina support as submicroscopic particles (<0.5 nm) or is atomically dispersed. However, since only limited parts of the catalyst actually have been studied, the possibility of large rhenium agglomerates can not be ruled out.

Samples 4 and 5 were dried in nitrogen atmosphere at 550 and 680°C, respectively, prior to reduction. The average diameter of the metal particles observed was 1.8 nm for sample 4 and 2.3 nm for sample 5 compared to 0.9–1.0 nm for samples 1, 2, and 3 which were dried in air prior to
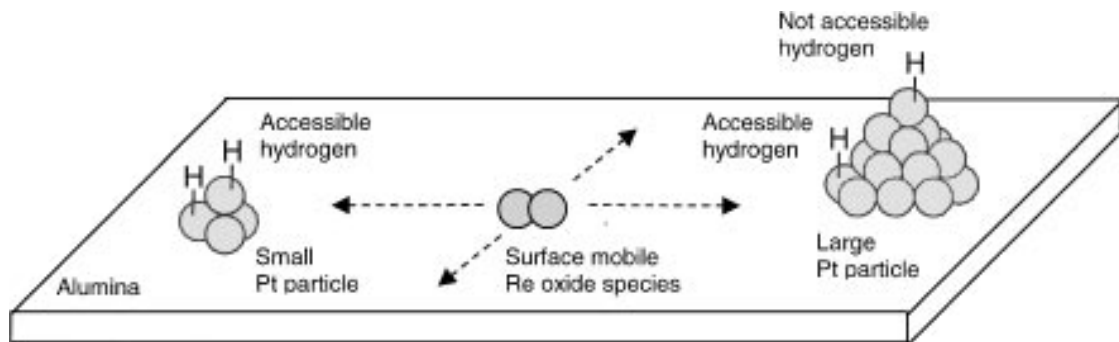
FIG. 10. Hydrogen accessibility for rhenium oxide reduction and bimetallic particle formation at platinum particles of different sizes.

reduction (Table 2). Thus, the pretreatment in nitrogen seems to have caused metal sintering. The previous TPR-analysis (13) suggested that platinum is reduced by decomposition of the platinum oxide precursor in the lack of oxygen at high temperature. During this decomposition process, which was found to start from temperatures of 400°C and higher, sintering does occur. The EDX-analyses of particles in samples 4 and 5 show mean values of 94 and 96% platinum, respectively. The low degrees of Pt–Re interaction observed in these samples may originate from "trapping" of the rhenium on the surface due to rhenium oxide decomposition during the pretreatment, reducing its mobility on the surface. Alternatively, the hydrogen accessibility necessary for rhenium oxide reduction and bimetallic formation on these larger platinum crystallites will be reduced due to a larger number of nonsurface platinum atoms and because part of the adsorbed hydrogen may be out of range for the surface mobile rhenium species (Fig. 10). Following this suggestion, only the smallest detectable metal particles (the representative ones) of a reforming catalyst are bimetallic (Figs. 5, 6, 7) while larger particles (2 nm and larger) will consist mainly of platinum metal (Figs. 8, 9). This explains the discrepancy between the conclusions of this work and the opposite conclusions regarding Pt–Re interaction drawn by Huang *et al.* (16). The 2–3 nm metal particles examined by these authors were possibly too large to allow formation of bimetallic particles, while the representative small Pt–Re bimetallic particles were not detected. The drying conditions (air 400°C) used in their study were something in between the drying conditions for sample 2 (air 240°C) and sample 3 (air 550°C) in the present work; thus bimetallic particles were most likely formed. Their low reduction temperature of 400°C (compared to 480°C in this work) may have contributed to the lower degree of rhenium reduction at Pt–Re interaction as well.

CONCLUSIONS

Evidence for platinum–rhenium interaction in small metal particles of the reduced catalyst has been established using combined STEM/EDX instrumentation. The degree of Pt–Re interaction is highly dependent on the conditions employed during pretreatment of the catalyst. The highest degree of Pt–Re interaction is obtained if the catalyst contains sufficient amounts of moisture prior to catalyst reduction. If the catalyst is dehydrated prior to reduction, less Pt–Re interaction occurs. The part of rhenium which is not associated with platinum is possibly distributed on the surface of the alumina support as submicroscopic particles.

On the basis of previous investigations it is evident that hydrogen chemisorption capacity and hydrogenolysis activity can effectively be used as probe techniques for Pt–Re interaction. Increased degree of Pt–Re interaction decreases the hydrogen uptake while increasing the activity for methane production. High-temperature nitrogen treatment of the catalyst in its oxidized state leads to platinum oxide decomposition, platinum sintering, and a low degree of Pt–Re interaction.

REFERENCES

1. Kluksdahl, H. E., U.S. Patent 3,415,737 (1968).
2. Bertolacini, R. J., and Pellet, R. J., *in* "Catalyst Deactivation" (B. Delmon and G. F. Froment, Eds.), p. 73. Elsevier, Amsterdam, 1980.
3. Yermakov, Y. U., and Kuznetsov, B. N., *J. Mol. Catal.* **9**, 13 (1980).
4. Burch, R., and Mitchell, A., *Appl. Catal.* **6**, 121 (1983).
5. Joyner, R. W., and Shpiro, E. S., *Catal. Lett.* **9**, 239 (1991).
6. Betizeau, C., Leclercq, G., Maurel R., Bolivar, C., Charcosset, H., Frety, R., and Tournayan, L., *J. Catal.* **45**, 179 (1976).
7. Biloen, P., Helle, J. N., Verbeek, H., Dautzenberg, F. M. and Sachtler, W. M. H., *J. Catal.* **63**, 112 (1980).
8. Shum, V. K., Butt, J. B., and Sachtler, W. M. H., *J. Catal.* **96**, 371 (1985).
9. Ribeiro, F. H., Bonivardi, A. L., Kim, C., and Somorjai, G. A., *J. Catal.* **150**, 186 (1994).

10. Augustine, S. M., Alameddin, G. N., and Sachtler, W. M. H., *J. Catal.* **115**, 217 (1989).
11. Pieck, C. L., Marecot, P., Querini, C. A., Parera, J. M., and Barbier, J., *Appl. Catal.* **133**, 281 (1995).
12. Prestvik, R., Ph.D. thesis, Norwegian Institute of Technology, Trondheim, 1995.
13. Prestvik, R., Moljord, K., Grande, K., and Holmen, A., *J. Catal.* **174** (1998).
14. Isaacs, B. H., and Petersen, E. E., *J. Catal.* **85**, 1 (1984).
15. Augustine, S. M., and Sachtler, W. M. H., *J. Catal.* **116**, 184 (1989).
16. Huang, Z., Fryer, J. R., Park, C., Stirling, D., and Webb, G., *J. Catal.* **148**, 478 (1994).
17. Lakis, R. E., Lyman, C. E., and Stenger, H. G., *J Catal.* **154**, 261 (1995).
18. Lyman, C. E., Goldstein, J. I., Williams, D. B., Ackland, D. W., von Harrach, S., Nicholls, A. W., and Statham, P. J., *Journal of Microscopy* **176**, 85 (1994).
19. Goldstein, J. I., Costly, J. L., Lorimer, G. W. and Reed, S. J. B., *Scanning Electron Microscopy/77* (O. Johari, Ed.), Vol. 1, p. 315. IITRI, Chicago, 1977.